ELSEVIER

Surface Science 370 (1997) 190–200

surface science

Atomic and electronic structure of the corundum (0001) surface: comparison with surface spectroscopies

V.E. Puchin [a], J.D. Gale [b], A.L. Shluger [c], E.A. Kotomin [d], J. Günster [e], M. Brause [e], V. Kempter [e,*]

[a] *Institute of Chemical Physics, University of Latvia, 19 Rainis blvd., Riga, LV-1586, Latvia*
[b] *Department of Chemistry, Imperial College, South Kensington, London SW7 2AY, UK*
[c] *Centre for Materials Research, Department of Physics, University College London, Gower Street, London WC1E 6BT, UK*
[d] *Institute of Solid State Physics, University of Latvia, 8 Kengaraga, Riga, LV-1063, Latvia*
[e] *Physikalisches Institut der Technischen Universität Clausthal, Leibnizstraße 4, 38678 Clausthal-Zellerfeld, Germany*

Received 3 May 1996; accepted for publication 24 July 1996

Abstract

The electronic structure and geometry of the Al-terminated corundum (0001) surface were studied using a slab model within the ab-initio Hartree–Fock technique. The distance between the top Al plane and the next O basal plane is found to be considerably reduced on relaxation (by 0.57 Å, i.e. by 68% of the corresponding interlayer distance in the bulk). An interpretation of experimental photoelectron spectra (UPS He I) and metastable impact electron spectra (MIES) is given using the calculated total density of states of the slab and the projections to the atoms, atomic orbitals, and He 1s floating atomic orbital at different positions above the surface. Calculated projected densities of states exhibit a strong dependence on the relaxation of surface atoms. The good agreement of simulated and experimental UPS and MIES spectra supports the correctness of calculated surface relaxation.

Keywords: An initio quantum chemical methods and calculations; Aluminum oxide; Auger ejection; Insulating surfaces; Photoelectron emission; Single crystal epitaxy

1. Introduction

Alumina surfaces have been studied extensively because of their technological importance [1]. Theoretically, the simplest non-polar Al-terminated (0001) corundum surface was predicted to be the most stable ideal termination of the bulk structure [2,3]. Pioneering ab initio Hartree–Fock (HF) calculations using the minimal (STO-3G) basis set of atomic orbitals (AOs) have predicted a large inward displacement (relaxation) of the terminating layer of Al atoms (0.4 Å, or 48% of the Al–O interlayer spacing) [4]. Further calculations performed in the local density approximation (LDA) with pseudopotentials and a plane-wave basis set predicted an even larger relaxation of about 0.7 Å [5,6]. The surface relaxation obtained using a semi-empirical tight binding model [7] is in agreement with the LDA calculations, but the semi-empirical study predicts a strong decrease in ionicity of the surface-atom bonding, in contrast with ab initio results. Calculations using pair potentials based on the empirical shell model [3] predict the surface relaxation to be intermediate between the HF [4] and LDA [5] data.

* Corresponding author. Fax: +49 5323 723600; e-mail: kempter@physik.tu-clausthal.de

0039-6028/97/$17.00 Copyright © 1997 Elsevier Science B.V. All rights reserved
PII S0039-6028(96)00971-5

Thus different theoretical methods predict qualitatively similar relaxations, but with some quantitative disagreement. However, comparison of theoretical and experimental data to validate the surface structure is difficult because atomic positions are not measured directly by any technique. Furthermore, calculated surface models are idealized and often do not correspond to the surfaces studied experimentally, while the calculated surface properties are not those measured experimentally. In particular, UV photoelectron spectroscopy (UPS) and metastable impact electron spectroscopy (MIES) [8] measure energy spectra of electrons emitted due to sample interaction with UV light or metastable excited He atoms. They probe the electronic structure of the ground state of the sample at the surface, with MIES being sensitive only to the topmost surface atoms. In this paper we address the question of whether a theoretical analysis of these spectra can provide information regarding the surface geometric structure.

The incentive for this study comes from our recent combined experimental and theoretical study of the MgO(001) surface [9]. It has demonstrated that the UPS (He I) and MIES (He* 1s2s) spectra have quite different structures in the valence-band energy region. In particular, MIES exhibits only one peak, whereas UPS has an additional peak at higher electron binding energy, but with lower intensity in comparison to the main peak. Electronic structure calculations demonstrated that this difference can be attributed to the fact that the metastable He atoms approaching the surface interact mostly with the electrons localized on the surface O $2p_z$ AOs, which are oriented perpendicularly to the surface and thus are most extended into the vacuum. UPS, on the other hand, probes a few layers of atoms beneath the surface [10]. Therefore, comparative analysis of the UPS and MIES spectra provides more complete information. Due to various approximations, a direct comparison of the theoretical and experimental absolute peak energies is impossible. However, it was shown that the *shape* of the UPS and MIES spectra (the number of peaks, their relative positions and intensities) of the MgO(001) surface can be well approximated by the total density of states (DOS) of a thin crystalline slab and the DOS projected to the surface O $2p_z$ AOs (PDOS), respectively [9]. Moreover, the results of these calculations demonstrated that the shape of both DOS and PDOS is very sensitive to the surface relaxation. This leads to the possibility of extracting information on surface atomic structure through the comparison of DOS and PDOS calculated for different surface relaxations with the experimental spectra.

In this paper we explore the above possibility in more detail for the case of the alumina surface. UPS and MIES spectra of the corundum monocrystalline (0001) surface and corundum films on Al(111) and W(110) substrates have recently been published [11–13]. Unlike MgO these spectra are qualitatively similar, each having two peaks, which probably results from the more complicated crystalline structure. As discussed below, the films grown on W(110) are most probably Al-terminated (0001) corundum or (111) γ-Al_2O_3 structures. Therefore Al electronic states must contribute to the valence-band DOS [4], and the straightforward interpretation of electron spectra given for the simple ionic rocksalt-type insulators like MgO may not be valid for corundum.

We study the relationship between the atomic and electronic structure of the relaxed corundum (0001) surface and the UPS and MIES spectra. For this purpose we have optimized the surface geometry using a slab model within the periodic Hartree–Fock method using an extended basis set, and calculated total and projected DOS at the surface. A novel method is proposed for the comparison of MIES spectra with theory: in order to simulate in a direct way the projectile–surface interaction (via Auger deexcitation connected with electron emission), the DOS projected onto the floating 1*s* orbital of He atom above the surface is calculated and analyzed as a function of the He coordinates.

2. Theoretical method

2.1. Model

In order to model the experimental spectra we have used the same method as discussed in Ref. [9]

for MgO. Interpretation of UPS spectra for narrow-band ionic crystals is still not established. In general, the angular and energy distribution of emitted photoelectrons is defined by the joint density of states of the valence and conduction bands, which is influenced by the dipole selection rules for the optical transitions, photoelectron diffraction in the crystalline lattice and photoelectron scattering on the surface potential barrier. A theoretical model which accounts for all these effects has been applied recently for the simulation of LiF photoelectron angular distributions [14]. However, this model is based on the assumption that the valence-band hole in this material is delocalized, as is the case in metals and semiconductors. The electron–phonon interaction, which leads to the efficient hole localization and significant broadening of the photoelectron spectrum, is neglected. On the other hand, the mean free path of the photoelectrons in the ionic insulators is known to be much smaller than in semiconductors and metals [10], which increases the surface contribution to the UPS at low photon energies (He I). In this paper we do not develop a rigorous theory for the calculation of UPS spectra; we merely assume that the structure in the valence-band UPS (He I) spectra is proportional to the valence band DOS of the near-surface region. It was proved to be a good approximation in the case of MgO(100) surface [9] and we believe that this is also the case for Al_2O_3(0001).

In the MIES experiment the interaction of the He* probe atom with the surface takes place via the Auger de-excitation process along the entire trajectory in front of the surface. Thus with MIES only the surface DOS is sampled. The differential transition probability (as defined in Eq. (8) of Ref. [9]) is proportional to the surface DOS relevant for the interaction with He*. Under the present conditions, when the projectile moves with thermal kinetic energy, electron emission due to Auger de-excitation occurs on the incoming path of the trajectory at comparatively large distances (several atomic units, typically); the transition energy is not strongly influenced by the actual interaction potentials of the initial and final states. We have shown on several occasions [9,11] that under these conditions the MIES spectra simulated in the way described by Niehaus et al. [15] directly reflect the surface DOS used as an input for the simulation. Therefore in Section 4 we compare the MIES spectra directly with the relevant surface-projected DOS and UPS (He I) spectra with the DOS in the near-surface region.

It is crucial for the comparison between theory and experiment to model the structure of the experimentally studied surface as closely as possible. However, the structure of the alumina surface strongly depends on method of preparation. In this work we make the main comparison with thin alumina films grown on W(110) [11]. The LEED pattern measured for this film is the same as that for the epitaxial Al_2O_3 film on the very similar Ta(110) substrate (Fig. 3 of Ref. [16]). This means that the surface of the film studied in Refs. [11–13] has the same long-range order and crystallographic orientation. It can be related to either (0001) corundum or the (111) face of γ-Al_2O_3. The ion scattering spectrum presented in Ref. [16] shows about a 1:3 ratio between Al and O peak intensities. This implies the presence of Al at the top surface layer and rules out the possibility of surface termination with a close-packed O layer, which was observed for the epitaxial alumina film on NiAl(110) substrate [17].

The corundum structure differs from that of γ-Al_2O_3 by the stacking sequence of close-packed oxygen layers (... ABAB ... in corundum and ... ABCABC ... in γ-Al_2O_3). Both the film (which was produced experimentally) and the slab (which can be treated theoretically by ab-initio methods) are too thin to distinguish between the hexagonal faces of these two Al_2O_3 structures. Therefore, we believe that a slab model of the Al-terminated surface of bulk corundum is adequate for modeling the experimentally observed surface.

2.2. *Computational technique*

In order to obtain the DOS required for the comparison with experiment we proceed as follows: a slab of nine atomic layers parallel to the (0001) plane has been used to simulate the corundum surface terminated by an Al plane (Fig. 1). We neglect the surface reconstruction and thus assume that the slab conforms to the plane hexagonal

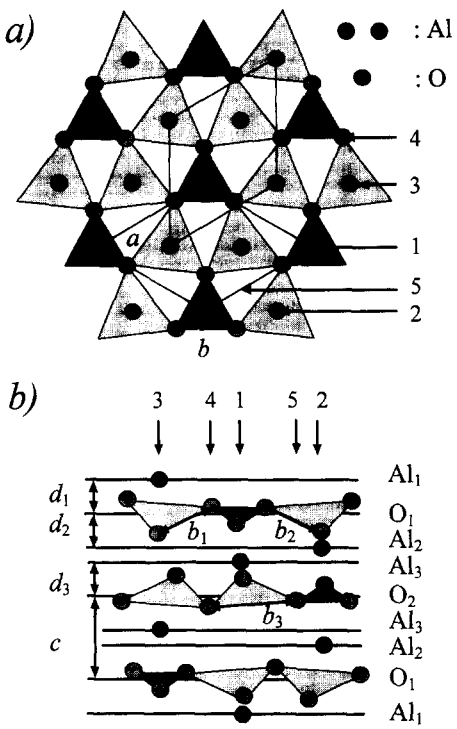

Fig. 1. The structure of a corundum (0001) slab of nine layers. Top (a) and side (b) views are given, where Al_1, Al_2, Al_3, O_1 and O_2 denote non-equivalent atoms. b_1, b_2, b_3, c, d_1, d_2 and d_3 are the seven independent geometric parameters optimized in the present study.

group P_{321} with a primitive unit cell containing 15 atoms. All the atoms within each of three O planes are equivalent and form a network of so-called *small* and *large* equilateral triangles. Three C_{2v} symmetry axes belong to the middle O plane and pass through the center of the small O triangle. In turn, C_{3v} axes are perpendicular to this plane and pass through the centers of both small and large O triangles. The primitive unit cell is a rhombus with side a, equal to the length of the translation vector.

In bulk corundum all the O planes are equivalent and separated by $c=2.166$ Å (see Fig. 1). Each plane can be transformed into the neighboring one by the combination of a 30° rotation around the C_{3v} axes and translation by $a/\sqrt{3}$, so that the two rhombic unit cells shown in Fig. 1a coincide. All Al atoms are situated on the C_{3v} axes. Each O plane is associated with two Al planes. Each Al atom is situated either above (black circles) or below (gray circles) the centers of large O triangles at a distance $d=0.838$ Å (see Fig. 1). Each Al atom in the bulk is surrounded by six O atoms forming three *short* bonds (1.857 Å) and three *long* bonds (1.969 Å).

On the (0001) surface, Al atoms have only three nearest O neighbors each. The position of an O atom within the middle plane is defined by one independent parameter. We use as this parameter the side of a large triangle (the distance between the O atoms forming the short bonds with the same Al atom) denoted as b in Fig. 1a. In the surface O layer, large triangles may differ in size due to the lack of the C_2 axes. Consequently, we need two parameters to define the positions of the O atoms within the surface plane. Since the slab has two non-equivalent O planes (O_1, O_2 in Fig. 1b) there are four independent parameters – b_1, b_2, b_3 and the distance c between planes. Three more independent parameters are the z coordinates of the Al planes: d_1, d_2, d_3 (Fig. 1b). In total this leads to seven independent parameters to be optimized.

The electronic structure and the total energy of the slab were calculated using the HF method as implemented in the CRYSTAL computer code [18]. In order to find the equilibrium atomic structure, the adiabatic potential energy surface was fitted to the quadratic form by means of the least square method. An 85-11G/8–411G basis set was used for Al and O, respectively. Accurate treatment of the oxide species requires a more extensive basis set than for aluminum as, if we take the oxide ion to be close to its formal charge state, the second electron is bound largely by the electrostatic potential, leading to increased diffuseness at the surface. We employed the Al and O Gaussian basis sets which have been optimized for bulk corundum by Mackrodt et al. [19]. A standard value of 0.35 au was used for the additional Al d-polarization function.

As far as the single-crystal surface is considered, it would be consistent to use for the slab calculations the lattice parameter found for the bulk structure by the same computational technique. The value of the a parameter optimized for the bulk corundum by Salasco et al. [4] using the HF

method is 0.5% less than the experimental one. This error has been attributed to the incompleteness of the basis set [4]. However, in the case of a thin film, the lattice spacing parallel to the surface is influenced by the substrate periodicity and could differ substantially from the bulk value. For instance, the average O spacing derived from the LEED pattern of a thin Al_2O_3 film on a Ta(110) substrate [16] is larger by 9% than that in the bulk of the corundum single crystal. The Ta lattice constant is 6% larger than that of W, and thus we expect the lattice spacing in the film on W(110) to be smaller and close to the experimental bulk value. Complicated film–substrate interface effects should be taken into account for an ab-initio estimate of the lattice parameter of the film. As a compromise we have used in our calculations the bulk experimental value of $a = 4.760$ Å.

The total and projected DOS were calculated for three distinct geometries: (i) the unrelaxed slab, (ii) that corresponding to the minimum of the slab total energy with respect to the seven independent coordinates mentioned above (b_1, b_2, b_3, d_1, d_2, d_3 and c), and (iii) that predicted by LDA calculations [5]. The HF method was used for the DOS calculation in all three cases, since it has been demonstrated previously [9] that the HF and LDA methods give practically the same electron density distribution and DOS for the same geometry of the slab. The calculated DOS is convoluted with a Gaussian function in order to account for the phonon broadening of the electron emission spectra. A value of 1 eV was chosen for the width of the Gaussian, because it gives the best agreement between the DOS and UPS spectrum. Mulliken population analysis has been used to calculate effective atomic charges for all atoms and bond populations for the nearest pairs of atoms. The DOS projected to the floating 1s Slater-type orbital with an exponential value of 1.69 au has been also calculated (see below) in order to simulate the He* metastable atom approaching the surface.

3. Results of calculations

Structural parameters for the three considered atomic configurations of the slab are summarized in Table 1. The top surface layer of Al atoms has the largest displacement with respect to the bulk position. The inward relaxation value of 68% of the Al–O bulk interlayer distance is 20% larger than the previous HF result [4]. This difference can be attributed to the more extended basis set and to the larger number of degrees of freedom taken into account in the minimization procedure. Further extension of the basis set with d-polarization functions on Al increases this relaxation by 5%. However, our relaxation is still smaller by 17% than that obtained in the above-mentioned LDA calculations. This discrepancy may be partially attributed to the particular choice of the Al core pseudopotential in LDA calculations, which probably underestimates Al–O repulsion at short distances. Also, the inclusion of correlation through the use of a density functional will favor increased surface compactness due to the resulting higher electron density.

The surface relaxation energy, defined as the difference in total energies of relaxed and unrelaxed slabs, was obtained to be 6.23 eV per unit cell. The energy of the atomic configuration suggested by LDA calculations is 0.57 eV higher than our minimum. Three-quarters of the relaxation energy gain is due to the inward displacement of the Al_1 (d_1 coordinate). This displacement is accompanied by the slight enlargement of the nearest O_1 triangle. Conversely, the size of the large triangle in the middle O plane decreases while the Al_3 atom moves away from it (increase of the d_3 coordinate). The displacements of Al atoms in general are considerably larger than those of O atoms. This is because the O sublattice forms an almost close-packed structure which is rather rigid.

The effective atomic charges (Table 1) confirm the high ionicity of corundum. Charges and bond populations of the central atoms (O_2, Al_3) are close to those in the bulk material. The atomic charges are sensitive to the basis set used. In the work of Salasco et al. [4], who initially used a 6–21G basis set, the charge on aluminum was close to +2.0. The addition of polarization functions to oxygen was found to have negligible effect, while including them at the metal centre greatly decreases the ionic character. Gale et al. [20] found that improving the oxygen basis by using an 8–411G set lead to

Table 1
The corundum slab energetics, charge distribution and bond populations as obtained for three different geometries; notations are given in Fig. 1

Atomic configuration of the slab	Unrelaxed	HF minimum	LDA minimum
Coordinates (Å)			
a	4.760	4.760	4.747
b_1	2.866	2.871	2.902
b_2	2.866	2.738	2.718
b_3	2.866	2.836	2.805
d_1	0.838	0.267	0.112
d_2	0.838	0.833	0.840
d_3	0.838	1.020	1.020
c	2.166	2.121	2.119
Energy per unit cell			
Total (au)	−2126.323585	−2126.552722	−2126.531606
Relaxation (eV)	0.0	6.23	5.66
Effective atomic charges (e)[a]			
Al_1	2.323	2.331	2.314
O_1	−1.590	−1.546	−1.508
Al_2	2.426	2.398	2.378
Al_3	2.500	2.476	2.456
O_2	−1.652	−1.710	−1.749
Bond populations (e)[b]			
Al_1–O_1	0.137	0.133	0.129
Al_2–O_1	0.079	0.074	0.081
Al_2–O_2	0.049	0.055	0.049
Al_3–O_1	0.041	0.057	0.062
Al_3–O_2	0.068	0.057	0.054

[a] The effective charges in the bulk are −1.64 e (O) and +2.46 e (Al).
[b] The Al–O bond populations in the bulk are 0.067 e (short bond) and 0.052 e (long bond).

Al charges of +2.25 for the bulk. The results in Table 1 are consistent with the trend of increasing ionic character as the basis set becomes more flexible.

For the unrelaxed surface there is a significant decrease in the aluminum charge for the top layer of the slab. However, during optimization this drop in ionic character is partially reversed. The final charges of both O and Al atoms in the middle of the slab are 0.15 e larger than those on the surface, while the Al–O bond population on the surface is doubled with respect to the middle layer. This demonstrates the increase in covalency at the corundum surface.

The calculated valence-band width is 9.5 eV, taking into account the phonon broadening. It is the same for the bulk corundum and for all considered atomic configurations of the slab. However, the electron binding energy depends on the surface relaxation. The main maximum in the total valence-band DOS of the slab is found at 6.2 eV below the vacuum level for the non-relaxed slab, at 11.5 eV for the HF-optimized geometry and 13.8 eV for the atomic configuration predicted by LDA calculations. The value of 9.0 eV has been found for the bulk, assuming that the vacuum level of the infinite crystal (zero of the energy) corresponds to the average electrostatic potential. Such an energy shift of the occupied electron bands due to the truncation of the conditionally converged Madelung potential sum is common for the surfaces of ionic crystals. It does not affect the DOS and electron density in the bulk of the crystal or in the middle of a sufficiently thick slab. However,

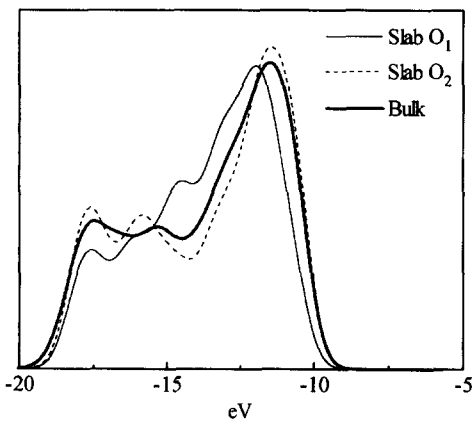

Fig. 2. Total and projected DOS for the bulk corundum and for a nine-layer slab, respectively. The heavy solid curve represents the total DOS of the bulk, whereas light curves correspond to the slab DOS projected to the surface oxygen (solid curve) and that from the middle layer (dashed curve).

it governs the average exponential decay of the electronic wavefunctions and the density above the surface. The HF method is known to overestimate the surface electron binding energy; LDA, on the other hand, always gives values which are too small and, consequently, a longer tail of the surface electron density into the vacuum.

Fig. 2 shows the slab DOS projected to the surface O atom (O_1) and to that in the middle of the slab (O_2), along with the bulk DOS. An energy shift of 2.5 eV has been applied to the bulk DOS in order to match the positions of the bulk and slab valence bands. The difference between the bulk and O_2 projected DOS is small. It is expected to vanish for the deeper O layers beneath the surface. The shift of the main peak in the O_1 projected DOS with respect to the O_2 projected and bulk DOS indicates band bending at the surface of about 0.5 eV. It is interesting to note that a similar shift, but with opposite sign, has been calculated for the MgO(100) surface [9].

The total DOS and that projected to the p_z orbital of the surface O atom are shown in Fig. 3 for three atomic configurations of the slab. The energy scale corresponds to the HF energy minimum; the two other curves are shifted so as to match the positions of the main peaks. As in the case of MgO, the main peak is close to the top of the band and is more pronounced in the projected

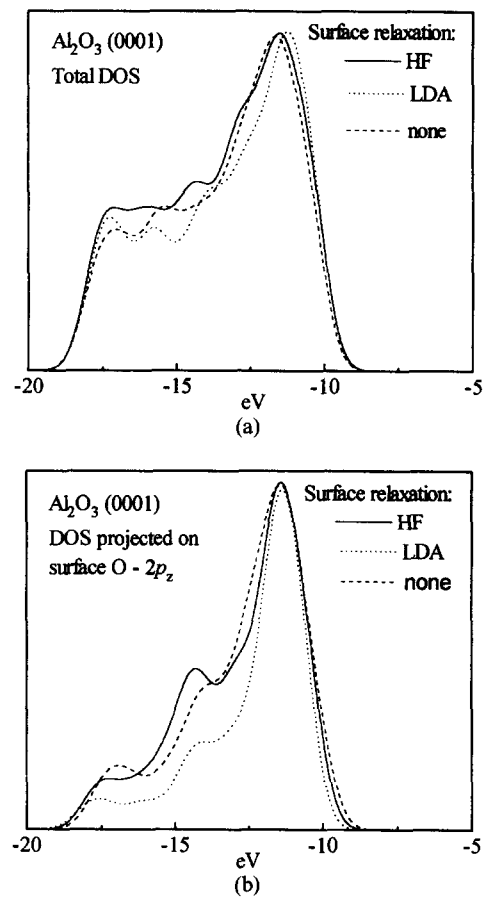

Fig. 3. Calculated total DOS of the slab (a) and that projected to the p_z orbital of the surface O atom (b). Three atomic configurations of the slab correspond to the unrelaxed surface (dashed curve), the HF-optimized geometry (solid curve) and the LDA-predicted geometry (dotted curve).

rather than in the total DOS. The total DOS has a pronounced shoulder at the high-energy side of the spectrum (between 13 and 17 eV). The projected DOS displays two additional peaks at the larger binding energy side separated from the main peak by 3 and 6 eV, respectively. The perturbation induced by the surface relaxation, which is mainly associated with inward motion of the surface Al atom, is not linear. The displacement of the surface Al atom by 0.57 Å from its perfect lattice position into the HF minimum leads to the slight increase in the relative intensity of the second peak and a similar decrease of the third peak (see Fig. 3b). However, its further displacement by only 0.12 Å,

as predicted by LDA calculations, decreases the intensity of both peaks roughly by a factor of 2. The magnitude of the effect of the surface relaxation is much larger in the projected DOS than in the total DOS.

In contrast to the flat and fully ionic MgO(100) surface, for corundum (0001) the terminating Al plane lies above the O plane, and Al–O bonds are partially covalent. Thus one intuitively expects that the interaction of the incident He* metastable with surface Al atoms and/or surface Al–O bonds could give a sizable contribution to the MIES spectrum. The spectrum of the emitted electrons may depend on the incident He* coordinate along the surface. In order to simulate this dependence, we have calculated the DOS projected to the floating He 1*s* orbital as a function of its coordinates. We find that the shape of this DOS does not depend on the distance from the surface (vertical *z* coordinate) while its magnitude decreases exponentially in the range $z = 2$–4 Å, reflecting the average behavior of the overlap integral between the floating AO and surface wave function.

In Fig. 4 we show the results for $z = 2.1$ Å, which is close to the typical distance where Auger de-excitation of the He* projectile takes place. We have considered five distinct horizontal positions of the floating orbital shown by arrows 1–5 in Fig. 1: 1 – He* above small O triangle, 2 – above large O triangle, 3 – above Al atom, 4 – above O atom, and 5 – above next-layer O atom. The corresponding projected DOS are shown in Fig. 4a. Fig. 4b shows their weighted average, which is to be compared with MIES spectrum. The weights of the individual contributions were taken as three for the points 4 and 5, and as unity for three other points (1–3), because the latter belong to the C_{3v} symmetry axes. Such a superposition corresponds to the approximate integration of the He 1s projected DOS over the plane parallel to the surface, because the chosen points (1–5) form an almost uniform hexagonal net. The dotted curve in Fig. 4b was calculated for the slab geometry predicted by the LDA method.

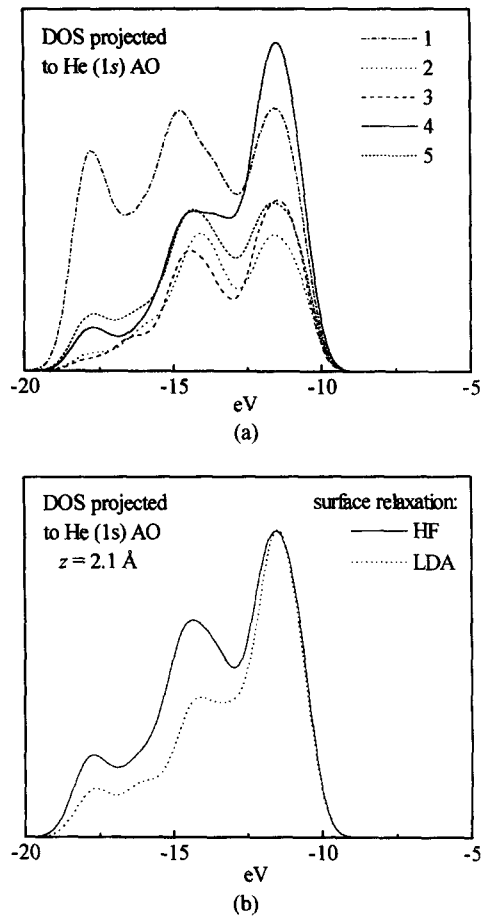

Fig. 4. Calculated DOS projected to the floating 1*s* AO, simulating an He atom at a distance 2.1 Å above the Al layer terminating the surface. Curves 1–5 in (a) correspond to the HF-optimized geometry of the slab and He situated above the center of small O triangle (1), large O triangle (2), surface Al atom (3), surface O atom (4) and next-layer O atom as shown by arrows in Fig. 1. The weighted average of these five curves, which simulates the MIES spectrum, is given in (b) for HF (solid curve) and LDA (dotted curve) surface relaxations.

4. Comparison with experiments

The experimental MIES and UPS measured in Refs. [11–13] are reproduced in Figs. 5a and 5b, respectively. The spectra represented by light solid lines were obtained from corundum films grown by coadsorbing Al and O_2 molecules onto a W(110) substrate held at 750 K [11]; the film thickness was estimated as 13 Å. Electron energies are given with respect to the vacuum level. The value of 3.8 eV for the surface work-function of the film was determined from the UPS spectra.

MIES and UPS spectra were also reported for Al(111) exposed to O_2 at room temperature [12].

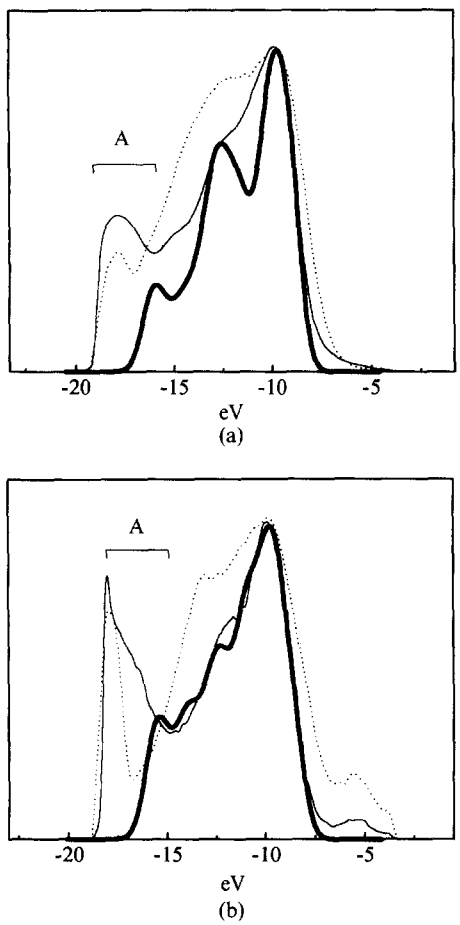

Fig. 5. The experimental MIES (a) and UPS (b) spectra for corundum films produced by coadsorption of Al and O_2 on a W(110) substrate (thin curves). Heavy curves show the result of theoretical simulations of MIES and UPS. They are equal to the light solid curves of Figs. 4a and 2, respectively. In the energy region denoted "A", the experimental spectra are affected by the secondary electron emission. The energy scale corresponds to the experimental electron binding energy. Dotted curves are the experimental spectra for a monocrystalline corundum sample.

After this oxygenation procedure they do not yet display the pronounced shoulder at $E \approx 12.3$ eV, but only an asymmetry of the main peak around $E = 9.8$ eV is seen. However, after annealing the interface stepwise up to 850 K, both the MIES and UPS spectra become virtually identical in the valence band (VB) region with those obtained by the coadsorption procedure [13]. For this reason these data are not reproduced here.

The MIES and UPS spectra represented by dotted lines were obtained for a corundum single-crystal (0001) surface [13]. In order to prevent the surface from charging-up positively (by the electrons leaving the surface during the ionization process), it was irradiated by low-energy ($h\nu = 6$ eV) photons. In both the MIES and UPS spectra of the corundum single-crystal (0001) surface the VB structure exhibits the two features discussed above, although the shape of the spectra differs in detail from that of the films. However, the effects of photons with sub-band-gap energies are not well studied at present. Because we cannot exclude that photon irradiation influences the surface structure to some extent, we consider these data as less reliable. For this reason, comparison between theory and experiment will be confined to the thin film data.

The MIES spectra show very little intensity above the top of the VB ($E > 7.6$ eV). We attribute the "soft tail" of the valence band emission to the ionization of such surface oxygen species which have a lower coordination than in the bulk, located at kinks, steps, etc. The VB emission consists of a pronounced peak ($E = 9.8$ eV) and a shoulder ($E \approx 12.3$ eV) towards higher binding energies.

The UPS spectra show the same two VB features ($E = 9.8$ and 12.3 eV). The weak intensity above the top of the VB is not well understood at present: it may be due to emission from the underlying substrate and/or from point defects located underneath the surface.

The high-energy part of both spectra above 16 eV is known to be affected by the emission of secondary electrons. Thus, this energy region (denoted "A" in Fig. 5) will not be interpreted here.

The results of theoretical calculations are given by heavy lines in Figs. 5a and 5b: the He 1s projected DOS at 2.1 Å above the surface (solid curve of Fig. 4b) is plotted along with the experimental MIES spectra and surface projected DOS (light solid curve of Fig. 2), along with UPS data. One-electron bands calculated using the HF method are known to have lower energies that experimental bands due to lack of electron correlation [21]. There is also uncertainty in the Fermi energy in the experimental spectra due to surface charging and other effects [10]. Therefore, in

Fig. 5, theoretical curves are shifted by 1.7 eV in order to match the experimental top of the VB.

In contrast to the MgO(100) surface and to the MgO film on Si(100) [9], the MIES and UPS spectra for the corundum surface show no large differences. Both spectra show two peaks ($E=9.8$ and 12.3 eV), while for MgO the MIES spectra show only the main peak which exhibits some asymmetry towards larger binding energies. The calculations reveal that this is a consequence of a smaller difference in corundum (as compared with MgO) between the parallel ($2p_x$) and perpendicular ($2p_z$) components of the O 2p projected DOS. It is directly related to the difference in the local symmetry and coordination numbers for surface oxygen atoms in MgO and corundum. Moreover, the surface oxygen layer in corundum is close-packed and does not contain cations (Al) at all, whereas the MgO(100) surface contains an equal number of anions and cations. This accounts qualitatively for the clear difference in the MIES and UPS spectra for these two kinds of oxides.

The calculated surface DOS is in good agreement with the UPS spectra (Fig. 5b). This confirms that the photoemission spectrum at He I incident-photon energy is mainly dependent on the initial state electron wavefunction. The final-state effects, including the dispersion of the conduction band and photoelectron scattering at the surface potential barrier, might be important for larger photon energies and angle-resolved UPS interpretation, but are probably less important in our case.

As can be seen from Fig. 2, the bulk DOS differs from the surface DOS, and therefore gives a worse agreement with UPS spectra. This could mean that the photoelectron scattering length in the crystal is extremely small (~ 2 Å) and the contribution from the bulk electronic states to the UPS is negligible at He I photon energies. However, the rather small difference between surface and bulk DOS does not allow us to make a definite conclusion about the escape depth of the photoelectrons.

The relative positions of the peaks in the DOS projected to the surface O $2p_z$ AO (see Fig. 2b) are in agreement with those in the MIES spectrum. However, the magnitude of the second peak is too low. The result of the MIES spectra simulation with the He 1s orbital as a probe of the surface DOS is much closer to the experiment (see Fig. 5a). However, the peaks in the experimental spectra are broader than in the simulated one, as was also the case in MgO. Three possible explanations have been suggested for this discrepancy [9]:

(1) The wider peaks reflect the influence of the surface roughness or the presence of surface imperfections, such as point defects, steps, kinks, etc.

(2) The wider O 2p structure is caused by the different interaction of the probe atom with the surface before and after the electron emission.

(3) The phonon broadening of MIES may be different from that for UPS due to the difference in the relevant hole relaxation energies and/or the phonon frequencies.

As can be seen from Fig. 4b, the second peak in the simulated MIES spectrum at the LDA geometry has significantly less intensity relative to the HF geometry, thus giving less satisfactory agreement with experimental spectrum.

From the comparison of the surface DOS and that projected to the 1s orbital of the He* projectile with the relevant UPS and MIES spectra (Fig. 5), respectively, it can be seen that the agreement between theory and experiment is satisfactory; the positions of the peaks and their relative magnitudes are similar. The comparison of the MIES spectrum with theoretical simulations allows us to discriminate between the HF- and LDA-optimized slab geometries in favor of that found in this paper using the HF technique.

5. Summary

The results of the present calculations demonstrate that in corundum, as in MgO, the shape, relative positions and intensities of the peaks in the surface density of electronic states (DOS) are in satisfactory agreement with the experimental He I photoelectron spectra (UPS). The metastable impact electron spectrum (MIES) arising from the Auger de-excitation of the He* metastable atom near the surface can be approximated by the DOS projected to a floating 1s atomic orbital (AO) which simulates the probing He atom. This method appears to be more accurate for the simulation of

the MIES spectra than utilization of just the DOS projected to the p_z AO of surface atoms used for MgO [9]. We also found that both DOS, strongly depend on the surface relaxation. This allows us to study details of the surface atomic structure by means of a comparison of the experimental MIES and UPS spectra with those simulated using ab initio methods. The present Hartree–Fock calculations predict an inward relaxation of the top Al layer as large as 68% of the Al–O interlayer distance. This slab geometry gives the surface projected DOS which is in best agreement with the experimental MIES and UPS spectra.

Acknowledgements

The authors are greatly indebted to the Deutsche Forschungsgemeinschaft for financial support through the grants Ke 155/24–1 and 436 LET 113/1. V.E.P. and E.A.K. have been partly supported by EC-HCM project No. ERB CIPDCT 940008. J.D.G. would like to thank the Royal Society for funding. We are grateful to N.E. Christensen for providing us with access to the CONVEX computer at Aarhus University (Denmark), to A. Svane for supplying us with the code for the least-square fitting to the quadratic form, and to M.J. Gillan for providing the equilibrium atomic configuration of the corundum slab, obtained with the LDA method.

References

[1] R.H. French and A.H. Heuer. J. Am. Ceram. Soc. 77 (1994) 292.
[2] P.W. Tasker, Adv. Ceram. 10 (1988) 176.
[3] W.C. Mackrodt, J. Chem. Soc., Faraday Trans. 2 85 (1989) 541.
W.C. Mackrodt, Philos. Trans. R. Soc. A 341 (1992) 301.
[4] C. Pisani, M. Causà, R. Dovesi and C. Roetti, Prog. Surf. Sci. 25 (1987) 119;
M. Causà, R. Dovesi, C. Pisani and C. Roetti, Surf. Sci. 215 (1989) 259;
L. Salasco, R. Dovesi, R. Orlando, M. Causà and V.R. Saunders, Mol. Phys. 72 (1991) 267.
[5] I. Manassidis, A. De Vita and M.J. Gillan, Surf. Sci. 285 (1993) L517;
I. Manassidis and M.J. Gillan, J. Am. Ceram. Soc. 77 (1994) 335.
[6] C. Kruse, M.W. Finnis, V.Y. Milman, M.C. Payne, A. De Vita and M.J. Gillan, J. Am. Ceram. Soc. 77 (1994) 431.
[7] T.J. Godin and J.P. LaFemina, Phys. Rev. B 49 (1994) 7691.
[8] G. Ertl and J. Küppers, in: Low Energy Electrons and Surface Chemistry (VCH, Weinheim, 1985) ch. 5.
[9] D. Ohs, W. Maus-Friedrichs, M. Brause, J. Günster, V. Kempter, V Puchin, A. Shluger and L. Kantorovich, Surf. Sci. 365 (1996) 557.
[10] V.E. Henrich and P.A. Cox, The Surface Science of Metal Oxides (Cambridge University Press, Cambridge, 1994).
[11] A. Hitzke, J. Günster, J. Kolaczkiewicz and V. Kempter, Surf. Sci. 318 (1994) 139.
[12] J. Günster, A. Hitzke, M. Brause, Th. Mayer and V. Kempter, Nucl. Instrum. Methods B 100 (1995) 411.
[13] J. Günster, Dissertation, TU Clausthal, 1996.
[14] E.L. Shirley, L.J. Terminello, J.E. Klepeis and F.J. Himpsel, Phys. Rev. B 53 (1996) 10296.
[15] P.A. Zeijlmans van Emmichhoven, P.A.A.F. Wouters and A. Niehaus, Surf. Sci. 195 (1988) 115;
P. Eeken, J.M. Fluit, A. Niehaus and I. Urazgil'din, Surf. Sci. 273 (1992) 160.
[16] P.J. Chen and D.W. Goodman, Surf. Sci. 312 (1994) L767.
[17] R.M. Jaeger, H. Kuhlenbeck, H.-J. Freund, M. Wuttig, W. Hoffmann, R. Franchy and H. Ibach, Surf. Sci. 259 (1991) 235.
[18] C. Pisani, R. Dovesi and C. Roetti, Hartree–Fock Ab-initio Treatment of Crystalline Systems, Lecture Notes in Chemistry, Vol. 48 (Springer, Heidelberg, 1988); R. Dovesi, V.R. Saunders and C. Roetti, CRYSTAL-92 User Manual, QCPE program no. 577 (Bloomington, Indiana, 1989).
[19] W.C. Mackrodt, to be published.
[20] J.D. Gale, C.R.A. Catlow and W.C. Mackrodt, Modelling Sim. Mater. Sci. Eng. 1 (1992) 73.
[21] A.B. Kunz, Phys. Rev. B 26 (1982) 2056.